Supplementary Materials

Parallel processing of nociceptive and non-nociceptive somatosensory information in the human primary and secondary somatosensory cortices: evidence from dynamic causal modelling of fMRI data

(Journal of Neuroscience 2011 31(24):8976-85)

M Liang[1], A Mouraux[2], GD Iannetti[1]

[1]*Department of Neuroscience, Physiology and Pharmacology, University College London, United Kingdom.* [2]*Institute of Neuroscience (IoNS), Université catholique de Louvain, Belgium.*

Supplementary Methods

DCM and BMS analyses based on different region of interest (ROI) selection strategies.

The lack of difference between the estimated functional connectivity of S1 and S2 during the cortical processing of nociceptive and non-nociceptive somatosensory input could be due to the fact that the ROIs defining S1, S2 and the thalamus were selected using the statistical conjunction maps, and, hence, that the ROIs were biased towards selecting only those voxels which exhibited a response to *both* nociceptive and non-nociceptive stimuli. This approach to define the ROIs was mandatory, as only models comprising the exact same brain areas can be compared using BMS in a valid way (Stephan et al., 2010). In order to examine whether our results could have been affected by this selection of voxels, we repeated the DCM and BMS analysis using two different sets of ROIs. The first set of ROIs was selected solely on the basis of the activation maps elicited in response to non-nociceptive stimulation whereas the second set of ROIs were selected solely on the basis of the activation maps elicited in response to nociceptive stimulation.

Control analysis 1. DCM and BMS analysis on models built using ROIs defined by non-nociceptive activation maps.

The three ROIs (i.e., the contralateral thalamus, S1 and S2) were composed solely by the voxels responding to non-nociceptive stimulation. The strategy of localizing each ROI and extracting the time series of each ROI was the same of that described in the main text. The coordinates of the maxima of the three ROIs at group level and in each participant are shown in Supplementary Table S1. Both the definition of the model families and the DCM and BMS procedure were identical to what performed in the main analysis.

Control analysis 2. DCM and BMS analysis on models built using ROIs defined by nociceptive activation maps.

The three ROIs (i.e., the contralateral thalamus, S1 and S2) were composed solely by the voxels responding to nociceptive stimulation. The strategy of localizing each ROI and extracting the time series of each ROI was the same of that described in the main text. The coordinates of the maxima of the three ROIs at group level and in each participant are shown in Supplementary Table S2. Both the definition of the model families and the DCM and BMS procedure were identical to what performed in the main analysis.

DCM and BMS analyses based on two more complex models.

It is important to highlight that our results were obtained using a very simple three-region model structure. In order to test the reliability of our results across more complex models (i.e., models including a larger number of brain regions), we performed two additional DCM and BMS analyses, in which a fourth ROI was added to the model. In the first analysis, the additional ROI encompassed the contralateral insula, whereas, in the second analysis, it encompassed the ipsilateral S2. These additional regions were chosen because they are well known to respond to both nociceptive and non-nociceptive stimuli (Porro, 2003; Apkarian et al., 2005; Tracey and Mantyh, 2007; Bjornsdotter et al., 2009; Nebel et al., 2010).

Control analysis 3. DCM and BMS analysis on models built using four ROIs including contralateral thalamus, S1, S2 and insula.

In this control analysis, a fourth ROI corresponding to the contralateral insular cortex was added to the models. The strategy of localizing each ROI and extracting the time series of each ROI was the same of that described in the main text. The coordinates of the maxima of the insula ROIs at group level and in each participant are shown in Supplementary Table S3. Both the definition of the model families and the DCM and BMS procedure were identical to what performed in the main analysis.

Sixteen DCM model families (A to P) were defined to test the same set of competing hypotheses (Supplementary Figure S3). In all model families, six intrinsic connections were defined. The four intrinsic connections between the thalamus, S1 and S2 were the same as described in the main text. The two additional intrinsic connections, one from the thalamus to the insula and the other from the S2 to the insula, were defined based on previous knowledge (Apkarian et al., 2005; Kandel et al., 2010). The 16 model families differ in terms of how the connections between the thalamus and S1 and between the thalamus and S2 are modulated, i.e., whether each of the two connections are modulated by non-nociceptive stimuli, by nociceptive stimuli, by both stimuli or by neither of them. Each model family contains 256 single models that differ in how the other four connections (i.e., S1 to S2, S2 to S1, thalamus to insula and S2 to insula) are modulated. Therefore, 4,096 models (256 models x 16 families) were defined in each participant, resulting in 49,152 models in total (4,096 models x 12 participants). Since, for computational reasons, it was not possible to estimate all possible models, only the simplest model (in which all the other four connections *are not* modulated by *neither* nociceptive *nor* non-nociceptive input) and the most complex model (in which all the other four connections *are* modulated by *both* nociceptive *and* non-nociceptive inputs) in each

family, resulting in a total of 384 models (2 models x 16 families x 12 participants), were estimated. BMS was performed on the 16 model families twice (Supplementary Figure S4): first, the 16 simplest models were compared; second, the 16 most complex models were compared. Similar to what performed in the main analysis, the thalamus was set as the receiving area, and the driving input to the thalamus was formed by all stimuli, regardless of their sensory modality.

Control analysis 4. DCM and BMS analysis on models constructed with four ROIs including the contralateral thalamus, S1, S2 and the ipsilateral S2.

In this control analysis, a fourth ROI corresponding to the ipsilateral S2 was added into the models. The strategy of localizing each ROI and extracting the time series of each ROI was the same of that described in the main text. The coordinates of the maxima of the ipsilateral S2 ROIs at group level and in each participant are shown in Supplementary Table S3. Both the definition of the model families and the DCM and BMS procedure were identical to what performed in the main analysis.

Sixteen DCM model families (A to P) were defined to test the same set of competing hypotheses (Supplementary Figure S5). In all model families, six intrinsic connections were defined. The four intrinsic connections between the thalamus, S1 and S2 were the same as described in the main text. The two additional intrinsic connections between the contralateral and ipsilateral S2 areas were defined based on previous knowledge (Apkarian et al., 2005; Kandel et al., 2010). The 16 model families differ in terms of how the connections between the thalamus and S1 and between the thalamus and S2 are modulated, i.e., whether each of the two connections are modulated by non-nociceptive stimuli, by nociceptive stimuli, by both stimuli or by neither of them. Each model family contains 256 single models that differ in how the other four connections (i.e., S1 to S2, S2 to S1, contralateral S2 to ipsilateral S2 and ipsilateral S2 to contralateral S2) are modulated. Therefore, 4,096 models (256 models x 16 families) were defined in each participant, resulting in 49,152 models in total (4,096 models x 12 participants). Since, for computational reasons, it was not possible to estimate all possible models, only the simplest model (in which all the other four connections *are not* modulated by *neither* nociceptive *nor* non-nociceptive input) and the most complex model (in which all the other four connections *are* modulated by *both* nociceptive *and* non-nociceptive inputs) in each family, resulting in a total of 384 models (2 models x 16 families x 12 participants), were estimated. BMS was performed on the 16 model families twice (Supplementary Figure S6): first, the 16 simplest models were compared; second, the 16 most complex models were compared. Similar to what performed in the main analysis, the thalamus was set as the receiving area, and the driving input to the thalamus was formed by all stimuli, regardless of their sensory modality.

Supplementary Results

Control analysis 1. DCM and BMS analysis on models built using ROIs defined by non-nociceptive activation maps.

The group-level exceedance probabilities of all 16 model families are shown in the upper left panel of Supplementary Figure S1. One single family (family P) displayed an exceedance probability (0.75)

that was far greater than the exceedance probabilities of all other families. Indeed, the second highest exceedance probability, in the families H, was 0.05. Family P included all models in which both nociceptive and non-nociceptive somatosensory inputs change, in parallel, the connectivity both from the thalamus to S1 and from the thalamus to S2. The group-level exceedance probabilities of each of the 256 single models (sorted according to families from A to P) showed that all 16 models of the best family (family P) had higher exceedance probabilities (> 0.01) than the models belonging to all the other families (< 0.002) (lower panel of Supplementary Figure S1). The structure of the average model of the family P, obtained by averaging all 16 models in this family using BMA, is shown in the upper right panel of Supplementary Figure S1, together with the corresponding estimated parameters. The average model structure showed that the two forward connections from the thalamus to S1 and from the thalamus to S2 were strongly modulated by both nociceptive and non-nociceptive somatosensory inputs, whereas the two reciprocal connections between S1 and S2 were only weakly modulated by both types of external perturbations.

Control analysis 2. DCM and BMS analysis on models built using ROIs defined by nociceptive activation maps.

The group-level exceedance probabilities of all 16 model families are shown in the upper left panel of Supplementary Figure S2. One single family (family P) displayed an exceedance probability (0.66) that was far greater than the exceedance probabilities of all other families. Indeed, the second highest exceedance probability, in the families N, was 0.09. Family P included all models in which both nociceptive and non-nociceptive somatosensory inputs change, in parallel, the connectivity both from the thalamus to S1 and from the thalamus to S2. The group-level exceedance probabilities of each of the 256 single models (sorted according to families from A to P) showed that all 16 models of the best family (family P) had higher exceedance probabilities (> 0.01) than the models belonging to all the other families (< 0.002) (lower panel of Supplementary Figure S2). The structure of the average model of the family P, obtained by averaging all 16 models in this family using BMA, is shown in the upper right panel of Supplementary Figure S2, together with the corresponding estimated parameters. The average model structure showed that the two forward connections from the thalamus to S1 and from the thalamus to S2 were strongly modulated by both nociceptive and non-nociceptive somatosensory inputs, whereas the two reciprocal connections between S1 and S2 were only weakly modulated by types of external perturbations.

The two additional analyses, using ROIs selected from either non-nociceptive activation maps or nociceptive activation maps, produced similar results as those obtained using the conjunction ROIs (Supplementary Figure S1 and S2). Therefore, these additional results provide evidence that the strategy adopted for the selection of ROIs did not bias our results.

Control analysis 3. DCM and BMS analysis on models built using four ROIs including contralateral thalamus, S1, S2 and insula.

DCM and BMS analysis on models built using four ROIs (contralateral thalamus, S1, S2 and insula). The group-level exceedance probabilities of all 16 simplest models are shown in the upper left panel of Supplementary Figure S4. One single family (family P, both connections from the thalamus to S1

and to S2 are modulated in both nociceptive and non-nociceptive processing) displayed an exceedance probability (0.70) that was far greater than the exceedance probabilities of all other families. Indeed, the second highest exceedance probability, in the families H, was 0.07. The structure of the simplest model P is shown in the upper right panel of Supplementary Figure S4, together with the corresponding estimated parameters. Similarly, the group-level exceedance probabilities of all 16 most complex models are shown in the lower left panel of Supplementary Figure S4. One single family (family P, both connections from the thalamus to S1 and to S2 are modulated in both nociceptive and non-nociceptive processing) displayed an exceedance probability (0.69) that was far greater than the exceedance probabilities of all other families. Indeed, the second highest exceedance probability, in the families H, was 0.08. The structure of the most complex model P is shown in the lower right panel of Supplementary Figure S4, together with the corresponding estimated parameters.

Control analysis 4. DCM and BMS analysis on models constructed with four ROIs including the contralateral thalamus, S1, S2 and the ipsilateral S2.

The group-level exceedance probabilities of all 16 simplest models are shown in the upper left panel of Supplementary Figure S6. One single family (family P, both connections from the thalamus to S1 and to S2 are modulated in both nociceptive and non-nociceptive processing) displayed an exceedance probability (0.85) that was far greater than the exceedance probabilities of all other families. Indeed, the second highest exceedance probability, in the families H, was 0.04. The structure of the simplest model P is shown in the upper right panel of Supplementary Figure S6, together with the corresponding estimated parameters. Similarly, the group-level exceedance probabilities of all 16 most complex models are shown in the lower left panel of Supplementary Figure S6. One single family (family P, both connections from the thalamus to S1 and to S2 are modulated in both nociceptive and non-nociceptive processing) displayed an exceedance probability (0.84) that was far greater than the exceedance probabilities of all other families. Indeed, the second highest exceedance probability, in the families H, was 0.04. The structure of the most complex model P is shown in the lower right panel of Supplementary Figure S6, together with the corresponding estimated parameters.

The results of these two additional analyses provide further support to our conclusion. Indeed, even when more brain areas are added to the model, BMS consistently selects models in which the responses to nociceptive and non-nociceptive stimuli in S1 and S2 are mainly driven by direct parallel projections from the thalamus (Supplementary Figures S3 to S6).

Supplementary Tables

Table S1. MNI coordinates of ROIs selected from activation map of non-nociceptive stimulation at group and individual level

	S1	S2	Thalamus
Group	-12,-46,64	-54,-31,25	-12,-13,10
S01	-15,-46,64	-60,-28,22	-12,-16,10
S03	-9,-46,64	-63,-28,22	-12,-13,10*
S04	-12,-46,67	-60,-28,25	-12,-13,10*
S05	-6,-49,73	-48,-25,25	-12,-13,10*
S07	-9,-58,67	-63,-37,34	-12,-13,1
S08	-15,-43,73	-57,-34,16	-12,-13,10*
S09	-12,-46,64*	-57,-19,13	-12,-19,13
S10	-12,-52,64	-57,-34,25	-12,-16,4
S11	-15,-49,64	-51,-13,16	-12,-13,10
S12	-9,-46,64	-63,-28,22	-12,-13,10*
S13	-12,-46,76	-39,-31,31	-9,-10,13
S14	-15,-49,64	-51,-46,25	-6,-7,10

*No activation was found at the threshold of $p < 0.05$ (uncorrected) and cluster size > 5 voxels, therefore the group ROI was used for these six single-subject ROIs.

Table S2. MNI coordinates of ROIs selected from activation map of nociceptive stimulation, at group and individual level

	S1	S2	Thalamus
Group	-12,-52,67	-60,-28,28	-6,-13,13
S01	-15,-46,61	-60,-25,22	-12,-16,7
S03	-24,-40,70	-54,-28,19	-12,-10,10
S04	-15,-46,67	-57,-37,28	-6,-13,13*
S05	-12,-49,70	-48,-22,25	-9,-16,7
S07	-15,-52,67	-57,-40,31	-12,-16,7
S08	-15,-43,73	-63,-22,28	-3,-10,1
S09	-12,-52,67*	-57,-22,16	-12,-22,10
S10	-12,-52,67*	-57,-37,25	-6,-22,7
S11	-12,-40,67	-57,-13,16	-15,-19,7
S12	-9,-55,73	-60,-28,19	-6,-13,13*
S13	-6,-37,76	-57,-22,25	-12,-13,13
S14	-15,-49,67	-60,-22,19	-3,-10,13

*No activation was found at the threshold of $p < 0.05$ (uncorrected) and cluster size > 5 voxels, therefore the group ROI was used for these four single-subject ROIs.

Table S3. MNI coordinates of ROIs selected from conjunction map elicited in response to both nociceptive and non-nociceptive stimuli, at group and individual level

	Contralateral Insula (control analysis 3)	Ipsilateral S2 (contoral analysis 4)
Group	-39, -16, 4	54, -25, 16
S01	-39, -16, 4*	45, -28, 19
S03	-36, -19, 13	60, -22, 13
S04	-36, -16, 4	51, -19, 22
S05	-33, -10, 1	51, -25, 19
S07	-39, -19, 1	66, -25, 37
S08	-39, -13, 7	54, -19, 28
S09	-36, -19, 4	60, -10, 16
S10	-36, -16, -5	42, -25, 16
S11	-39, -13, 10	48, -25, 28
S12	-39, -16, 4*	54, -31, 25
S13	-39, -16, 4*	63, -31, 28
S14	-39, -19, -2	51, -22, 22

*No activation was found at the threshold of $p < 0.05$ (uncorrected) and cluster size > 5 voxels, therefore the group ROI was used for these three single-subject ROIs.
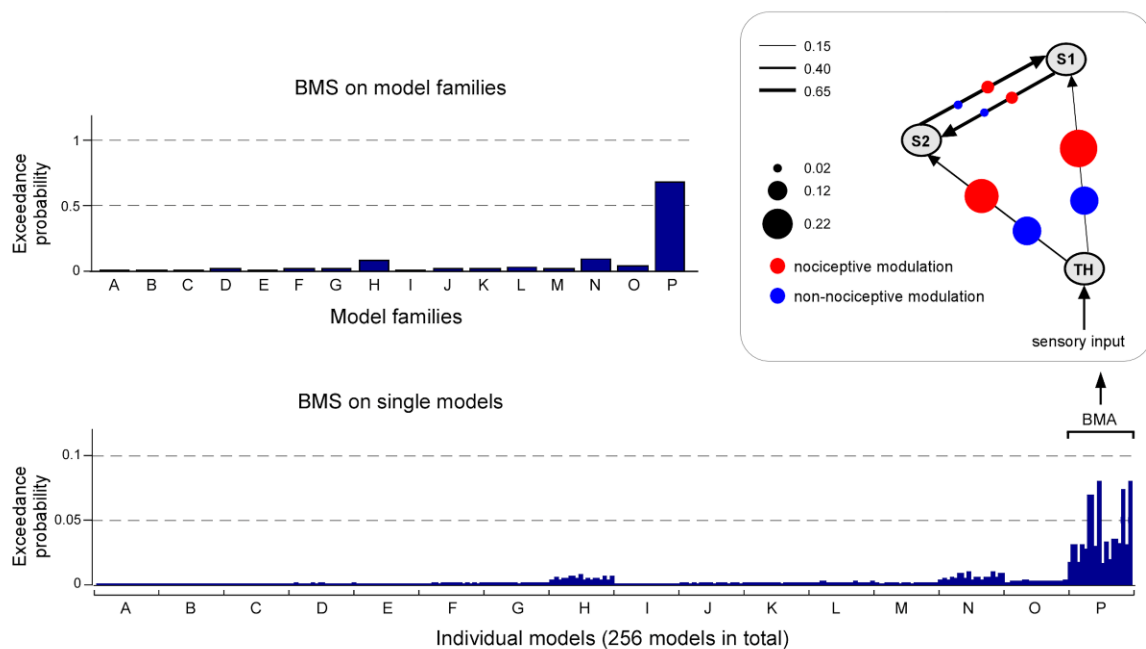
Supplementary Figures

Figure S1. The results of the Bayesian model selection (BMS) based on the DCMs constructed with the ROIs selected from the activation map of non-nociceptive stimuli. Upper left panel: the exceedance probabilities of all 16 model families (A to P) showed that the model family P (in which both connections from the thalamus to S1 and from the thalamus to S2 are modulated in both nociceptive and non-nociceptive processing) exceeds by far those of all the other model families. Lower panel: the exceedance probabilities of all single models (sorted according to model families) showed that the models in family P had always higher exceedance probabilities. Upper right panel: structure of the average model of the winning family P. The black lines with arrows represent the intrinsic connections between brain areas and the thickness of each line indicates the mean strength of each intrinsic connection across participants. The size of the red and blue dots on each connection represents the magnitude of the modulatory effect of nociceptive or non-nociceptive stimulation, respectively. This structure shows that the two forward connections from the thalamus to S1 and from the thalamus to S2 were strongly modulated by both nociceptive and non-nociceptive somatosensory inputs, whereas the two reciprocal connections between S1 and S2 were only weakly modulated by both types of inputs.
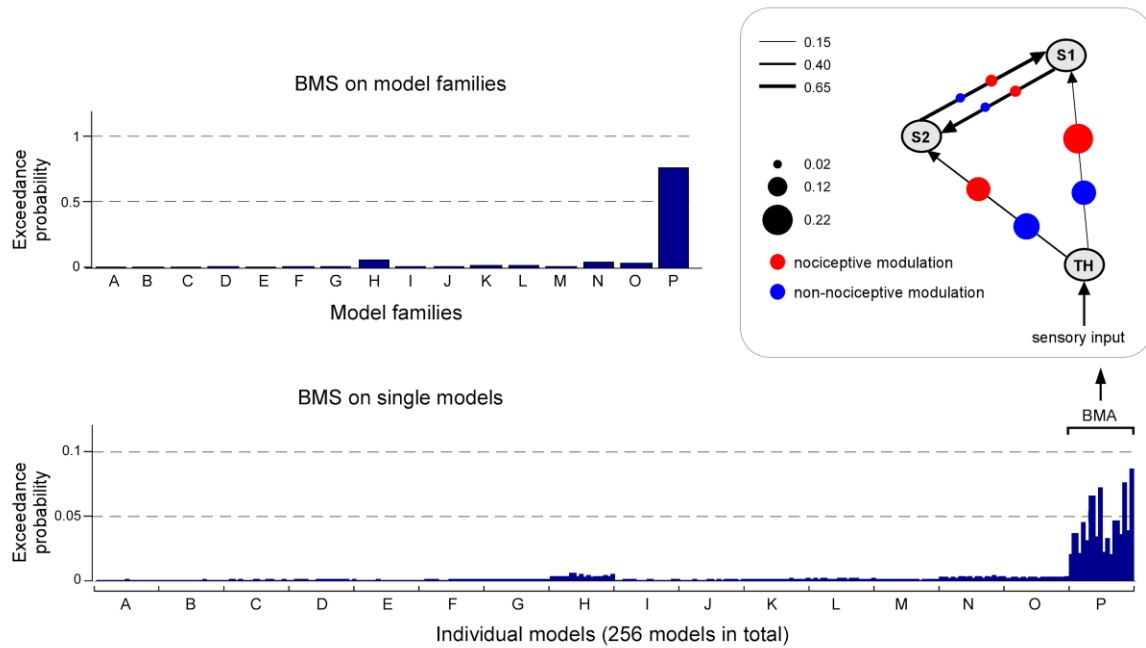
Figure S2. The results of the Bayesian Model Selection (BMS) based on the DCMs constructed with the ROIs selected from the activation map of nociceptive stimuli. Upper left panel: the exceedance probabilities of all 16 model families (A to P) showed that the model family P (in which both connections from the thalamus to S1 and from the thalamus to S2 are modulated in both nociceptive and non-nociceptive processing) exceeds by far those of all the other model families. Lower panel: the exceedance probabilities of all single models (sorted according to model families) showed that the models in family P had always higher exceedance probabilities. Upper right panel: structure of the average model of the winning family P. The black lines with arrows represent the intrinsic connections between brain areas and the thickness of each line indicates the mean strength of each intrinsic connection across participants. The size of the red and blue dots on each connection represents the magnitude of the modulatory effect of nociceptive or non-nociceptive stimulation, respectively. This structure shows that the two forward connections from the thalamus to S1 and from the thalamus to S2 were strongly modulated by both nociceptive and non-nociceptive somatosensory inputs, whereas the two reciprocal connections between S1 and S2 were only weakly modulated by both types of inputs.
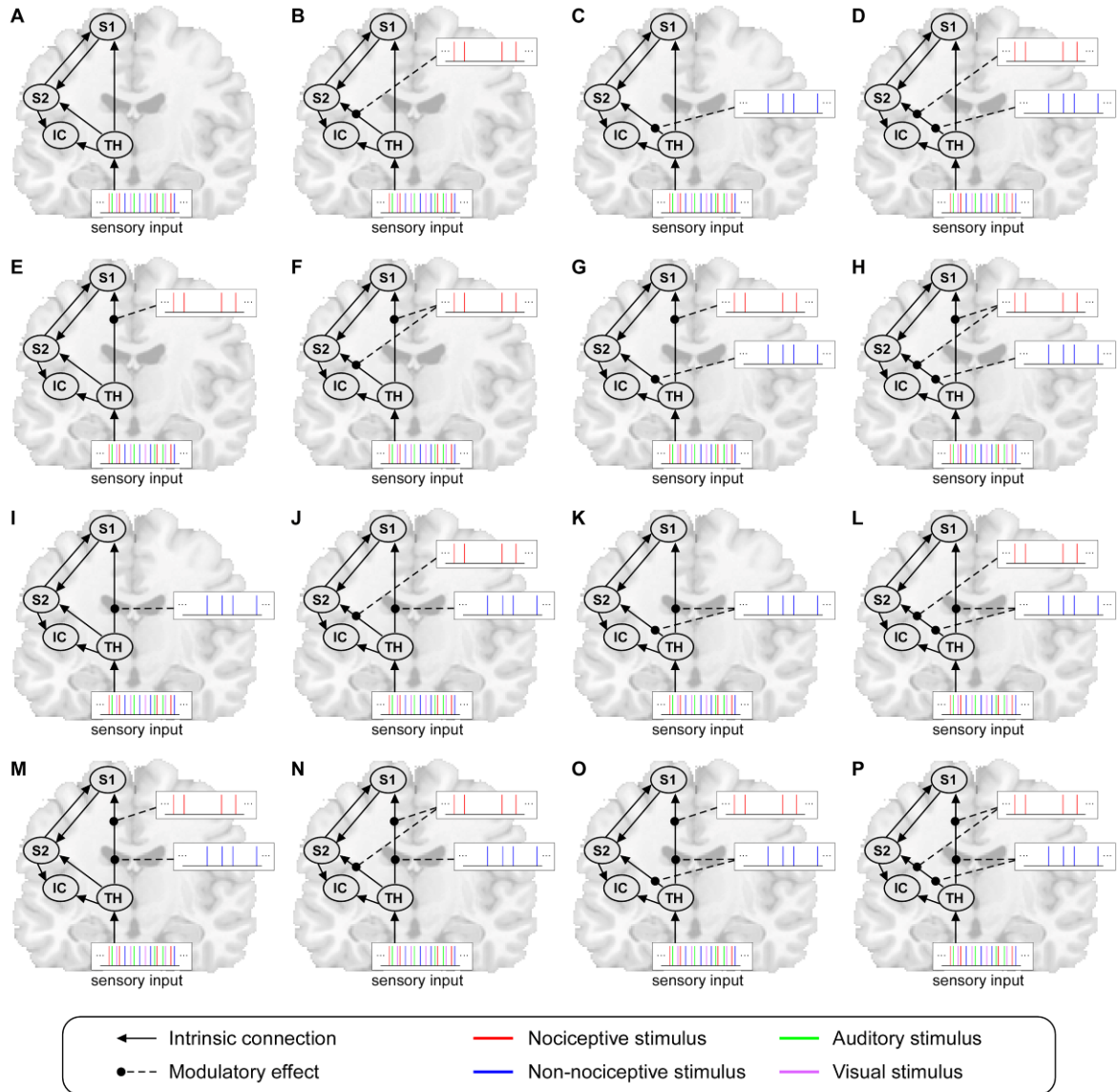
Figure S3. Structures of the sixteen DCM model families (A to P) with the contralateral insular cortex added to the main network. In all model families, six intrinsic connections were defined. These intrinsic connections are indicated by the black lines with arrows, and the arrows indicate the direction of the connectivity. The 16 model families differ in terms of how the connections between the thalamus and S1 and between the thalamus and S2 are modulated, i.e., whether each of the two connections are modulated by non-nociceptive stimuli, by nociceptive stimuli, by both stimuli or by neither of them. These modulations are indicated by the black dashed lines. The colour of the vertical lines at the end of the dashed lines indicates the modality of the stimuli that exert the modulatory effect. Each model family contains 256 single models (not shown) that differ in how the other four connections (i.e., S1 to S2, S2 to S1, thalamus to insula and S2 to insula) are modulated. The thalamus was set as the receiving area, and the driving input to the thalamus was formed by all stimuli regardless of their sensory modality. These stimuli are represented by vertical lines with different colours indicating different sensory modalities (red: nociceptive; blue: non-nociceptive; green: auditory; purple: visual). S1: primary somatosensory cortex; S2: secondary somatosensory cortex; TH: thalamus; IC: insular cortex.
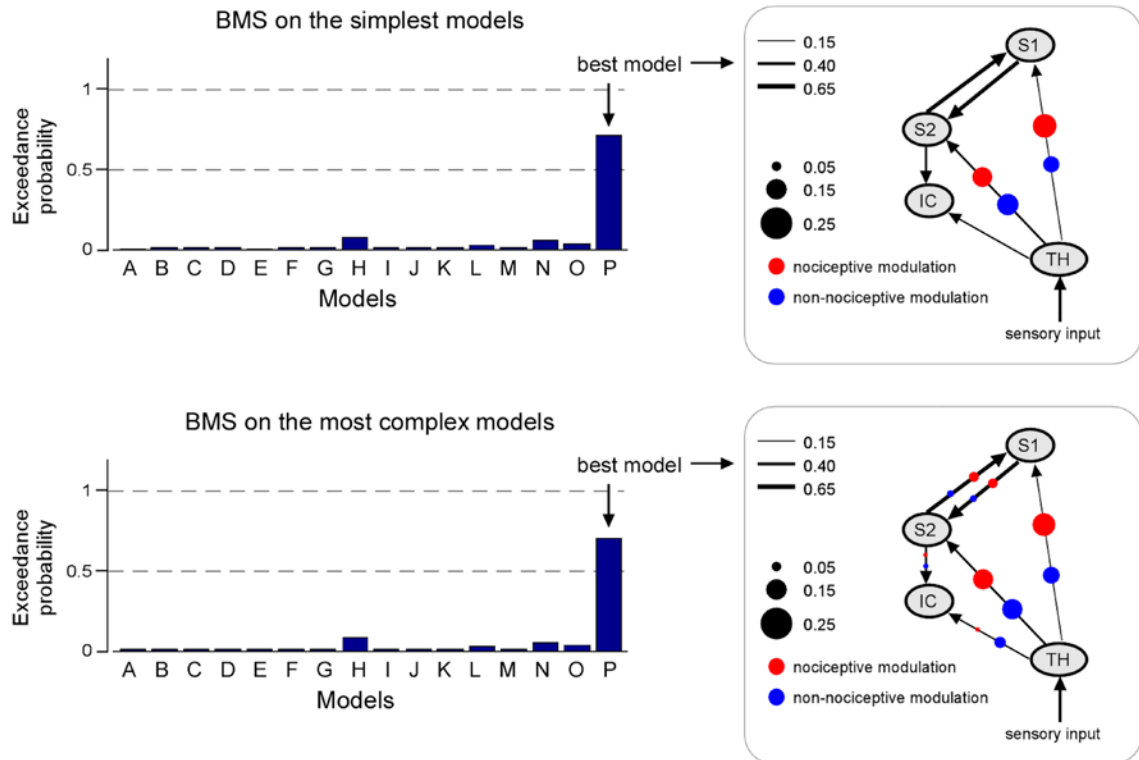
Figure S4. The results of the Bayesian model selection (BMS) on the models with the contralateral insular cortex included. Upper left panel: the exceedance probabilities of all 16 simplest models (A to P) showed that the model P (in which both connections from the thalamus to S1 and from the thalamus to S2 are modulated in both nociceptive and non-nociceptive processing) exceeds by far those of all the other models. Upper right panel: structure of the winning model P of all simplest models. Lower left panel: the exceedance probabilities of all 16 most complex models (A to P) showed that the model P (in which both connections from the thalamus to S1 and from thalamus to S2 are modulated in both nociceptive and non-nociceptive processing) exceeds by far those of all the other models. Lower right panel: structure of the winning model P of all most complex models. The black lines with arrows represent the intrinsic connections between brain areas and the thickness of each line indicates the mean strength of each intrinsic connection across participants. The size of the red and blue dots on each connection represents the magnitude of the modulatory effect of nociceptive or non-nociceptive stimulation, respectively. This structure shows that the two connections from the thalamus to S1 and from the thalamus to S2 are strongly modulated by both nociceptive and non-nociceptive inputs, while the other four connections are weakly modulated by both types of inputs.
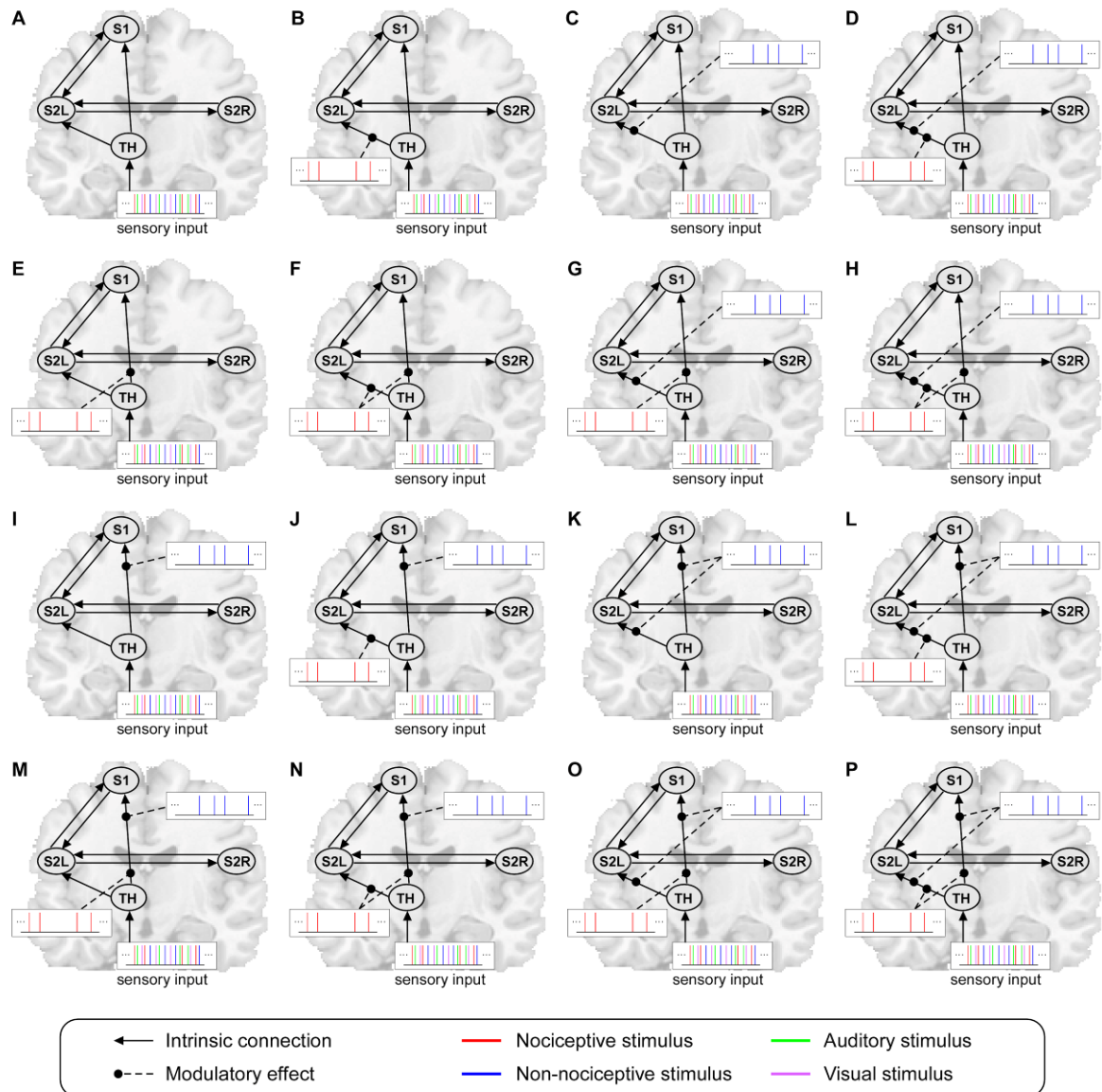
Figure S5. Structures of the sixteen DCM model families (A to P) with the ipsilateral S2 added to the main network. In all model families, six intrinsic connections were defined. These intrinsic connections are indicated by the black lines with arrows, and the arrows indicate the direction of the connectivity. The 16 model families differ in terms of how the connections between the thalamus and S1 and between the thalamus and S2 are modulated, i.e., whether each of the two connections are modulated by non-nociceptive stimuli, by nociceptive stimuli, by both stimuli or by neither of them. These modulations are indicated by the black dashed lines. The colour of the vertical lines at the end of the dashed lines indicates the modality of the stimuli that exert the modulatory effect. Each model family contains 256 single models that differ in how the other four connections (i.e., S1 to S2L, S2L to S1, S2L to S2R and S2R to S2L) are modulated (not shown). The thalamus was set as the receiving area, and the driving input to the thalamus was formed by all stimuli regardless of their modality. These stimuli are represented by vertical lines with different colours indicating different sensory modalities (red: nociceptive; blue: non-nociceptive; green: auditory; purple: visual). S1: primary somatosensory cortex; S2L: contralateral (left) secondary somatosensory cortex; S2R: ipsilateral (right) secondary somatosensory cortex; TH: thalamus.
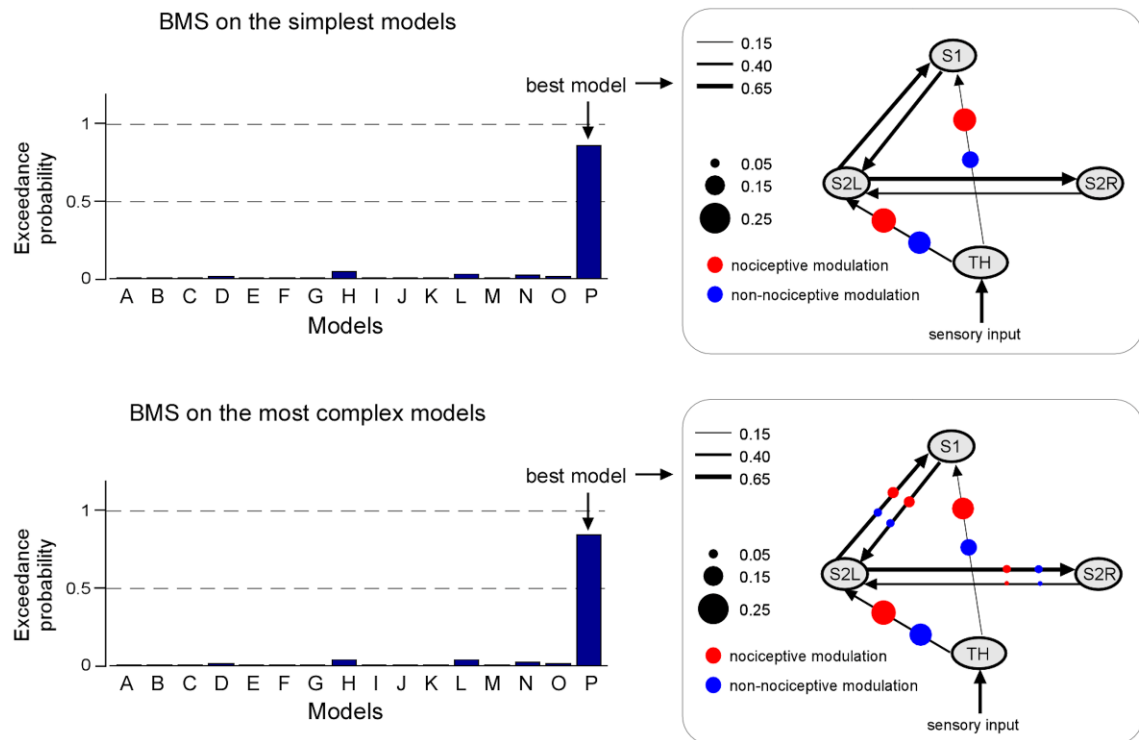
Figure S6. The results of the Bayesian model selection (BMS) on the models with the ipsilateral S2 included. Upper left panel: the exceedance probabilities of all 16 simplest models (A to P) showed that the model P (in which both connections from the thalamus to S1 and from the thalamus to S2 are modulated in both nociceptive and non-nociceptive processing) exceeds by far those of all the other models. Upper right panel: structure of the winning model P of all simplest models. Lower left panel: the exceedance probabilities of all 16 most complex models (A to P) showed that the model P (in which both connections from the thalamus to S1 and from the thalamus to S2 are modulated in both nociceptive and non-nociceptive processing) exceeds by far those of all the other models. Lower right panel: structure of the winning model P of all most complex models. The black lines with arrows represent the intrinsic connections between brain areas and the thickness of each line indicates the mean strength of each intrinsic connection across participants. The size of the red and blue dots on each connection represents the magnitude of the modulatory effect of nociceptive or non-nociceptive stimulation, respectively. This structure shows that the two connections from the thalamus to S1 and from the thalamus to S2 are strongly modulated by both nociceptive and non-nociceptive inputs, while the other four connections are weakly modulated by both types of inputs.

References

Apkarian AV, Bushnell MC, Treede RD, Zubieta JK (2005) Human brain mechanisms of pain perception and regulation in health and disease. Eur J Pain 9:463-484.

Bjornsdotter M, Loken L, Olausson H, Vallbo A, Wessberg J (2009) Somatotopic organization of gentle touch processing in the posterior insular cortex. J Neurosci 29:9314-9320.

Kandel ER, Schwartz JH, Jessell TM (2010) Principles of neural science, 5th Edition. New York, NY ; London: McGraw-Hill.

Nebel MB, Folger S, Tommerdahl M, Hollins M, McGlone F, Essick G (2010) Temporomandibular Disorder Modifies Cortical Response to Tactile Stimulation. J Pain.

Porro CA (2003) Functional imaging and pain: behavior, perception, and modulation. Neuroscientist 9:354-369.

Stephan KE, Penny WD, Moran RJ, den Ouden HE, Daunizeau J, Friston KJ (2010) Ten simple rules for dynamic causal modeling. Neuroimage 49:3099-3109.

Tracey I, Mantyh PW (2007) The cerebral signature for pain perception and its modulation. Neuron 55:377-391.